

ARTICLE

Topical Application of *Houttuynia cordata Thunb* Ethanol Extracts Increases Tumor Infiltrating CD8⁺/Treg Cells Ratio and Inhibits Cutaneous Squamous Cell Carcinoma *in vivo*

Lipeng Gao^{1,2,#}, Rongyin Gui^{1,#}, Xinnan Zheng¹, Yingxue Wang¹, Yao Gong¹, Tim Hua Wang¹, Jichuang Wang³, Junyi Huang^{1,2} and Xinhua Liao^{1,2,*}

¹School of Life Sciences, Shanghai University, Shanghai, 200444, China

²Shanghai Key Laboratory of Bio-Energy Crops, Plant Science Center, Shanghai University, Shanghai, 200444, China

³Institute for Translational Medicine, Fujian Medical University, Fuzhou, 350122, China

*Corresponding Author: Xinhua Liao. Email: xinhualiao@foxmail.com

#Lipeng Gao and Rongyin Gui contributed equally to this work

Received: 10 March 2022 Accepted: 28 June 2022

ABSTRACT

Houttuynia cordata Thunb (HCT) is a medicinal and edible herb that has beneficial effects on various diseases due to its diuretic, anti-inflammatory, anti-oxidative, anti-microbial, anti-viral, anti-cancer and anti-diabetic properties. Most reports of its anti-cancer activity were conducted *in vitro*, and its effects on cutaneous squamous cell carcinoma (SCC) have not been investigated yet. Using DMBA/TPA induced SCC mice model, we found that topical treatment by HCT, as well as its bioactive ingredient monomer, efficiently inhibited tumor growth. Mechanistically, tumor infiltrating CD4⁺, Foxp3⁺ T regulatory cells (Tregs) were significantly reduced and CD8⁺/Treg cells ratio was largely increased in tumors after HCT treatment. In addition, several chemokines which function to recruit immune cells were largely reduced in SCC cancer cells treated by HCT *in vitro*. Our results demonstrate the therapeutic effects of HCT on cutaneous SCC and indicate it might inhibit cancer through regulating tumor infiltrating lymphocytes and the tumor immune microenvironments.

KEYWORDS

Herba Houttuyniae; sodium new houttuynfonate; tumor infiltrating lymphocytes; tumor microenvironment

1 Introduction

Houttuynia cordata Thunb (HCT) is a well-known traditional Chinese medicinal and edible herb, which possesses a variety of pharmacological activities including diuretic, anti-microbial, anti-viral, anti-diabetic, anti-inflammatory, anti-oxidative, anti-mutagenic and anti-cancer properties [1,2]. It has shown therapeutic effect on many diseases including inflammation, pneumonia, severe acute respiratory syndrome (SARS), covid-19/SARS-CoV-2 [3,4], muscular sprain, cancer, obesity, stomach ulcer and cancer [1–2,5]. HCT has inhibitory effects on cell growth of colon cancer [6], gastric cancer [7], melanoma [8], hepatocellular carcinoma [9], breast cancer [10], colorectal cancer [11], lung cancer [12] and leukemia *in vitro* [13]. HCT also exhibits inhibitory activity on lung cancer *in vivo* [14]. However, it has not been studied in non-melanoma skin cancer yet.



This work is licensed under a Creative Commons Attribution 4.0 International License, which permits unrestricted use, distribution, and reproduction in any medium, provided the original work is properly cited.

Skin cancer is the most common cancer worldwide [15,16]. Basal cell carcinoma (BCC) and squamous cell carcinoma (SCC) are the most common forms of non-melanoma skin cancer. In comparison with BCC, SCC is more malignant and has the potential to recur and metastasize to other tissues and organs [15,16]. The incidence of SCC has increased over the past decades [15,17]. Diagnosis of squamous cell carcinoma is usually made with an incisional biopsy to assess the depth of invasion and other aggressive factors, such as poor grade of differentiation, desmoplasia, perineural invasion, presence of small tumor islands or tumor satellites [18,19]. Non-invasive technique reflectance confocal microscopy can provide horizontal skin images up to a 250 μm of maximum depth, representing a helpful aid for SCC diagnosis in the clinical practice [20–22]. Most SCC can be surgically removed. If the surgery is contraindicated or the tumor is located in a cosmetically sensitive areas, radiotherapy and chemotherapy may be used as adjuncts to surgery in patients with advanced SCC [23]. There is still a lack of safe and effective medicine for treating malignant SCC. Exposure to ultra-violet radiation is the most common cause of SCC. Other risk factors include exposure to radiation, carcinogenic chemicals, chronic skin ulceration, and immunosuppressive medication [24]. SCC development is a multistep process that consists of DNA mutation, genome instability, epigenetic changes, inflammation, oxidative stress and tumor microenvironment changes [24–27]. Mice SCC can be induced by two-stage carcinogenesis protocols which employ mutagenic chemical 7, 12-dimethylbenz[a]anthracene (DMBA) as initiators and proinflammatory chemical 12-O-tetradecanoylphorbol-13-acetate (TPA) as promoters [28]. This mouse model mimics human SCC exposed to UV or other carcinogens. Large-scale whole exon sequencing revealed that many DNA mutations induced by DMBA/TPA are consistent with mutations in human SCC [29]. In the mouse SCC model, tumors on back skin can be directly visualized, quantitatively measured and therefore traced individually over time. In addition, the drug can be topically applied onto the skin, therefore better reaching the tumor cells to execute its anti-cancer activity. It is well known that the metabolic rate of drugs in mice is 10 times that in humans [30]. Systematic application of drugs often shows no or mild activity in mice, owing to that the drugs could not reach the therapeutic concentration in blood. Traditional medicine usually uses whole plant extracts instead of monomers to treat diseases. They often only show mild to moderate therapeutic effects in humans, and these effects might not be observed in mice if they are systematically applied. Thus, chemical-induced mice SCC is an ideal model to evaluate the anti-cancer activity of traditional medicine by topical application.

Cancer cells grow in a special microenvironment where tumor-associated cells (immune cells, fibroblast, etc.) and cancer cells interact with each other to reach a balance between suppression and tolerance of cancer cells growth. Infiltrating immune cells are major constituents of the tumor microenvironment which play important roles in tumor development, invasion, metastasis, and outcome. Among these infiltrating cells, CD8^+ effector T cells are capable of killing cancer cells, while CD4^+ , Foxp3^+ T regulatory cells (Tregs or T_{reg} cells) secrete a variety of immunosuppressive cytokines, which dampen induction and proliferation of effector T cells [31]. Cancer cells alter the normal homeostatic ratio of effector to regulatory T cells and evade immune surveillance. High infiltrating CD8^+ /Treg cells ratios are associated with better prognosis and better response to chemotherapy and immunotherapy in various cancer types [32]. HCT can reduce tissue infiltrating inflammatory cells. In the rat carrageenan-air pouch model, oral administration of supercritical extracts of HCT suppressed carrageenan-induced exudation as well as inflammatory cell infiltration [33]. In influenza A virus-induced acute lung injury mice model, the lungs treated with flavonoid glycosides extracted from HCT presented milder inflammatory infiltration [34]. However, it has not been examined whether HCT treatment can alter the tumor-infiltrating lymphocytes and tumor immune microenvironment.

In this study, we used the mouse SCC model to examine the anti-cancer activity of HCT and one of its bioactive ingredients sodium new houttuuyfonate (SNH). We used chemical DMBA/TPA to induce SCC and then applied ethanol extracts of HCT or SNH onto the back skin. In comparison with the control group, the

SCC growth was significantly reduced without affecting the mice's body weight, indicating low toxic effects of HCT and SNH. Mechanistically, we found tumor-infiltrating CD8⁺ and CD4⁺ T cells were both reduced after HCT treatment. More significantly, the ratio of the CD8⁺/Treg cell was largely increased. Our data demonstrate that HCT is a potential drug for treating cutaneous SCC, and indicate it might inhibit tumor growth by regulating the tumor immune microenvironment.

2 Materials and Methods

2.1 Animals

ICR mice were obtained from Shanghai SLAC Laboratory Animal Co., Ltd. (China) and housed under SPF conditions. All experiments involving animals were performed in accordance with the guidelines of the Institutional Animal Care and Use Committee (IACUC) of Shanghai University (the Protocol Number: 2019033).

2.2 Materials

7, 12-dimethylbenz[a]anthracene (DMBA) and 12-O-tetradecanoylphorbol-13-acetate (TPA) were purchased from Sigma-Aldrich, Inc. Dried HCT whole plants were purchased from Jiangxi Qirentang Chinese Herbal Slices Co., Ltd. (China). Sodium new houttuuyfonate (SNH, purity $\geq 98\%$) was purchased from Shanghai Yuanye Bio-technology Co. Ltd. (China). Vendor and catalog information of antibodies against the following proteins are listed here: β -Catenin (#8480S, Cell Signaling Tech), Actin (#HC201, TransGen Biotech), ERK2 (#A0229, Abclonal Tech), ABCG2 (#A5661, Abclonal Tech), CD4 (for Western blot, #bs-0766R, Beijing Biosynthesis Biotech), CD8 (for Western blot, #bs-10699R, Beijing Biosynthesis Biotech); CD4 (conjugated with Alexa Fluor 700, for immunostaining, #56-0041-80, Thermo Fisher Scientific), CD8 (conjugated with Alexa Fluor 488, for immunostaining, #553-0081-80, Thermo Fisher Scientific), FoxP3 (conjugated with Alexa Fluor 488, for immunostaining, #126405, Biolegend).

2.3 Preparation of *Houttuynia cordata* Thunb Ethanol Extracts

The dried whole plants were grounded into powders, which were then immersed in 95% ethanol (3 mL of 95% ethanol per 1 g of powder) with stirring at room temperature overnight. The mixture was then centrifuged at $2800 \times g$ and filtered through Whatman filter paper. Finally, the ethanol extracts were lyophilized by a rotary evaporator. The final solid extracts were stored at -20°C . Before use, solid extracts were re-dissolved in organic solvent DMSO.

2.4 Mice Skin Carcinogenesis Model and Treatment

A two-stage model of skin tumorigenesis was employed to induce skin cancer. Back skins of 6-Week-old female ICR mice were shaved and then applied topically with DMBA (100 nmol/300 μL of acetone) twice weekly for two weeks, followed by TPA (10 nmol/300 μL of DMSO) twice weekly for six weeks. When tumor appeared, tumor length (L) and width (W) were measured twice a week by vernier caliper. The tumor volume (TV) was calculated according to the formula $\text{TV} = (\text{L} \times \text{W}^2)/2$. The total tumor volume of each mouse is the sum of all tumors on the back skin. When the average total tumor volume of each mouse reached $\sim 100 \text{ mm}^3$, 14 mice with similar total tumor volume were selected and divided into HCT treatment and control groups. The two groups had similar average total tumor volume and distribution. Thereafter, the mice were treated with HCT ethanol extracts or the control solvent daily by topical application for another three weeks. TPA would not be further applied during HCT treatment.

In addition, SNH was dissolved in 75°C ddH₂O as a 100 mg/kg stock solution and stored at 4°C . When the average total tumor volume of each mouse reached $\sim 100 \text{ mm}^3$, 27 mice with similar total tumor volume were selected and divided into SNH (20 mg/kg), SNH (100 mg/kg) and control groups. The three groups had similar average total tumor volume and distribution. Thereafter, the mice were treated with SNH or the control water daily by topical application for another five weeks. TPA would not be further applied during SNH treatment.

2.5 TPA-induced Skin Thickening in Mice

Back skins of 6-Week-old female ICR mice (N = 6) were shaved and pretreated with topical application of HCT ethanol extracts or the control solvent daily for 10 days, followed by TPA (10 nmol/300 μ L of DMSO) topical application daily for 3 days. The skin was then harvested for further analysis.

2.6 Western Blot Analysis of Tumor Samples

After three weeks of treatment, mice from HCT and control groups were euthanized and the tumors with similar volume were harvested by scissors. Tumor samples were grounded in liquid nitrogen and dissolved in RIPA lysates containing protease inhibitors. Samples were then sonicated and centrifuged. The supernatant was aspirated and mixed with SDS-loading buffer for further analysis. Protein samples (20–35 μ g) were resolved on 12% Tris-glycine gels and transferred onto a nitrocellular membrane. After blocking, the membrane was incubated with the primary antibody and then horseradish peroxidase (HRP)-conjugated secondary antibody. After washing, the HRP substrate was added and the chemiluminescence signal was detected by a CCD camera.

2.7 Hematoxylin and Eosin (H&E) Staining

Briefly, tumor samples were embedded in paraffin, sectioned and dewaxed. After samples were hydrated, they were stained with hematoxylin and eosin. The samples were dehydrated and then applied with Permount/Toluene solution, covered with a coverslip and sealed with nail polish. Images were captured using an optical microscope.

2.8 Immunostaining

Tumor samples were embedded and frozen on dry ice in OCT compound (Sakura Finetek) and then sectioned at 6–9 μ m. Sample sections were then fixed in 4% PFA and stained with Alexa Fluor conjugated antibodies. Fluorescence images were visualized and captured by fluorescent microscopy.

2.9 Real-Time Quantitative PCR

The total RNA of the human A431 cells was isolated with TRIzol (Ambion, USA) and reverse-transcribed to cDNA by an iScript Select cDNA Synthesis Kit (Bio-Rad, Hercules, USA). Real-time PCR was performed with iQ SYBR Green Supermix (Bio-Rad, Hercules, USA) and primers for IL-1 β , IL-6 and TNF- α (Tsingke Biotechnology Co., Ltd., China) and analyzed by the 2(-Delta Delta C(T)) method. β -actin served as the housekeeping gene. Real-time PCR was performed on an CFX 96 Real-time system (Bio-Rad, USA). The primer sequences are listed below: β -actin, CCCAAGGCCAACCGCGAGAAGAT and GTCCCGGCCAGCCAGGTCCAG; IL-1 β , CACGATGCACCTGTACGATCA and GTTGCTCCAT-ATCCTGTCCCT; IL-6 TACCCCAGGAGAAGATTCC and GCCATCTTTGGAAGGTTTCAG; TNF- α , GGCTCCAGGCGGTGCTTGTC and AGACGGCGATGCGGCTGATG.

2.10 Statistical Analysis

Statistical differences in data were evaluated with a two-tailed student's *T*-test or analysis of variance (ANOVA) by GraphPad Prism. The difference was considered to be significant when $P < 0.05$ (*), $P < 0.01$ (**), and $P < 0.001$ (***). Quantitative data were presented as mean \pm standard deviation.

3 Results

3.1 Topical Application of HCT Ethanol Extracts or Its Bioactive Ingredient Inhibits Tumor Growth

To prepare HCT ethanol extracts, we grounded the dry plant into powders, which were immersed in 95% ethanol to extract the soluble contents. The mixture was then centrifuged, filtered, lyophilized and weighed. The yield of ethanol extraction was 2.5% w/w. The product was then resuspended in DMSO to obtain a

41.67 mg/mL concentration, so that the final dose of 300 μ L of drug applied onto each mouse (\sim 25 g) would be 500 mg/kg.

To examine HCT anti-cancer activity, we used the two-stage model to induce SCC. Back skins of 6-week-old female ICR mice were shaved and then topically applied with DMBA twice weekly for two weeks, followed by TPA twice weekly for six weeks, the time point when the total tumor volume of most of the mice reached \sim 100 mm³. Mice with too small or large total tumor volume were excluded, and the left 14 mice with similar total tumor volume were selected and divided into HCT treatment and control groups. Thereafter, the mice were topically applied with 300 μ L of HCT ethanol extracts or solvent DMSO as control daily for another three weeks. TPA application would be stopped during drug treatment.

During treatment, the mice of both groups remained in similar good physical condition. The mice's body weight of the two groups occasionally fluctuated slightly during treatment, but the overall body weight of the mice remained unchanged (Figs. 1A and 1B). As revealed by tumor growth curves, HCT treatment significantly suppressed tumor growth (Figs. 1A and 1C). At the endpoint of treatment, the average total tumor volume of each mouse in the HCT group reached 637 mm³, which was much lower than that in the control group with 1041 mm³. In addition, the tumor number of the HCT group was lower than that of the control group, indicating HCT also suppressed the emergence of new tumors (Figs. 1A and 1D).

One of the main bioactive ingredients of HCT is sodium houttuynon (SH). Due to the chemical instability of SH, its adduct analog, sodium new houttuynon (SNH), has been synthesized to improve stability [35]. We then examined whether SNH had similar anti-cancer activity against SCC. As described above, mice with a total tumor volume of \sim 100 mm³ were divided into three groups and treated with 20 mg/kg SNH, 100 mg/kg SNH and control solvent, respectively. As revealed by tumor growth curves, SNH treatment also efficiently suppressed tumor growth as well as the number of new emerging tumors in a dose-dependent manner (Figs. 1E and 1F). The overall body weight of the three groups of mice showed no difference (data not shown). All of these data and observations demonstrate that topical application of the HCT extracts or its active ingredient efficiently suppresses SCC growth with low/no toxicity to the animals.

3.2 HCT Treatment Does not Change Known Cancer-Promoting Pathways

H&E staining showed similar architecture of tumor tissues with similar size harvested from HCT and control groups (Fig. 2A). To investigate the molecular mechanism of how HCT inhibits SCC, we examined whether some known cancer-promoting pathways were affected by HCT treatment. The protein β -Catenin is essential for skin cancer stem cell maintenance and SCC growth [36]. Western blot analysis showed that β -Catenin in the HCT treatment group was statistically lower than that of the control (Figs. 2B and 2C). However, there was huge variation between tumors even in the same group. Comprehensive genomic analysis of DMBA/TPA-induced SCC has revealed that the vast majority of SCC possesses mutations in Hras, Kras, or Rras2 [29]. Ras genes are often activated and play important roles during the early stages of squamous cell carcinoma development [37,38]. However, we did not observe the change of Ras downstream factor-ERK2 protein (Figs. 2B and 2C). The drug pump, ATP-binding cassette sub-family G member 2 (ABCG2), is well known as a specific marker of the "side population" (SP) of the cancer stem cells and is associated with drug resistance. ABCG2 could be controlled by several pathways, including the PI3K/Akt pathway [33]. ABCG2 protein expression varied between tumors, and there was no statistical difference between the HCT group and the control group (Figs. 2B and 2C). Since there was huge heterogeneity of protein expression between tumors, either in different mice or in different tumors from the same mice, it was difficult for us to obtain conclusive results. Therefore, we decided not to further pursue identifying signal pathways altered by HCT treatment.

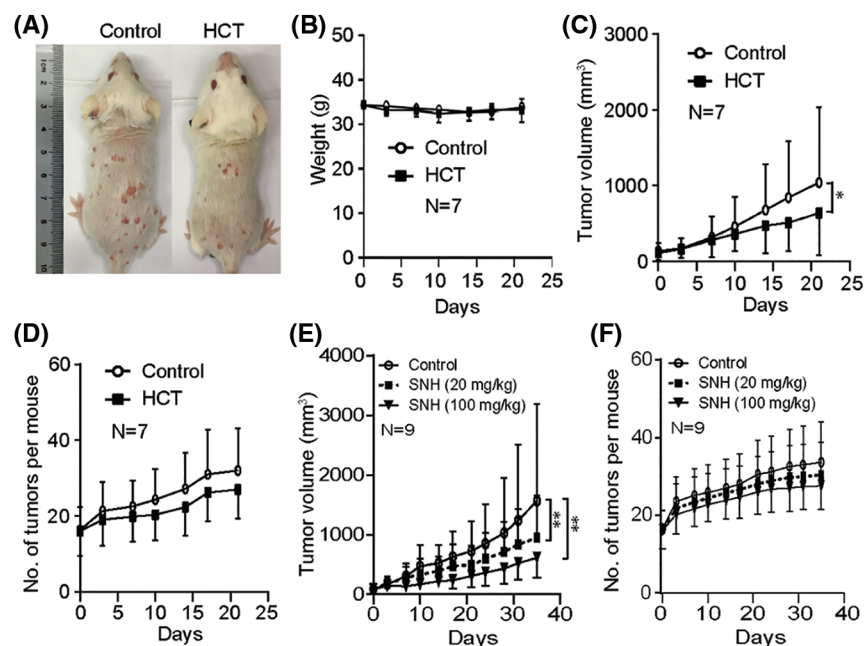


Figure 1: *Houttuynia cordata* Thunb ethanol extracts inhibit cutaneous SCC growth. Cutaneous SCC was induced by DMBA/TPA. When the total tumor volume of most of the mice reached $\sim 100 \text{ mm}^3$, HCT or solvent DMSO was topically applied onto the skin. Mice tumor volume and body weight were measured twice a week. (A) Representative images of back skin tumors in control and HCT groups. (B) Bodyweight of the HCT group and the control group over time. $P=0.294$. (C) The tumor growth curves of the HCT group and the control group. $P=0.038$. (D) Tumor number of the HCT group and the control group. $P=0.056$. (E) The tumor growth curves of the SNH (20 mg/kg) group, SNH (100 mg/kg) group and control group. $P=0.0087$ (20 mg/kg SNH group and control group). $P=0.0018$ (100 mg/kg SNH group and control group). (F) Tumor number of the SNH (20 mg/kg) group, SNH (100 mg/kg) group and control group. $P=0.480$ (20 mg/kg SNH group and control group). $P=0.079$ (100 mg/kg SNH group and control group). (*) represents $P < 0.05$. (**) represents $P < 0.01$

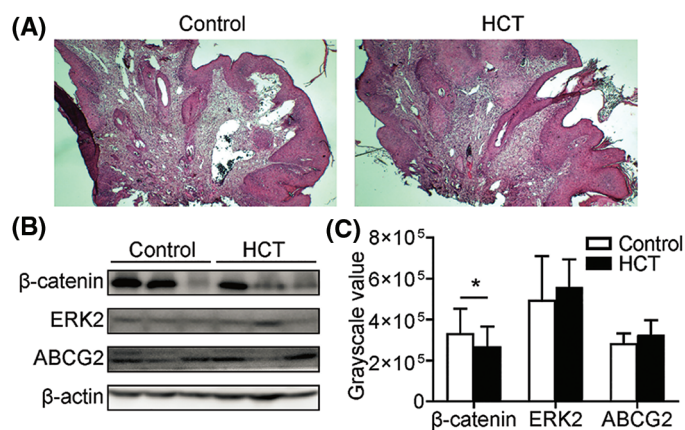


Figure 2: HCT treatment does not change known cancer-promoting pathways. (A) H&E staining of tumor samples with similar size harvested from HCT treatment or control group. (B) Proteins β -Catenin, ERK2, ABCG2 in tumors from HCT treatment or control group were analyzed by western blot. Actin was loaded as control. (C) Statistic quantification of western blot results. For β -Catenin, $P=0.020$; for ERK2, $P=0.020$; for ABCG2, $P=0.222$. (*) represents $P < 0.05$

3.3 Topical Pretreatment of HCT Ethanol Extracts Suppress Inflammation-Mediated Skin Thickening Induced by TPA

It has been reported that TPA alone could induce mouse ear skin edema and this model has been used as a test for anti-inflammatory activity [39,40]. Similar to ear skin, we found back skin swelling/thickening can be induced by TPA. To evaluate the anti-inflammatory activity of HCT, mice back skin was pretreated daily with topical application of HCT for 10 days, followed by TPA (10 nmol/300 μ L of DMSO) topical application daily for 3 days. The skin was then fixed by 4% PFA, embedded in paraffin, sectioned and followed by H&E staining. Both epidermal and dermal thickness were significantly decreased after HCT treatment (Figs. 3A–3D). Consistently, the proliferation of interfollicular epidermal (IFE) cells was also suppressed by HCT treatment (Figs. 3E and 3F). These results strongly indicates that HCT inhibits SCC by reducing skin inflammation and proliferation during carcinogenesis.

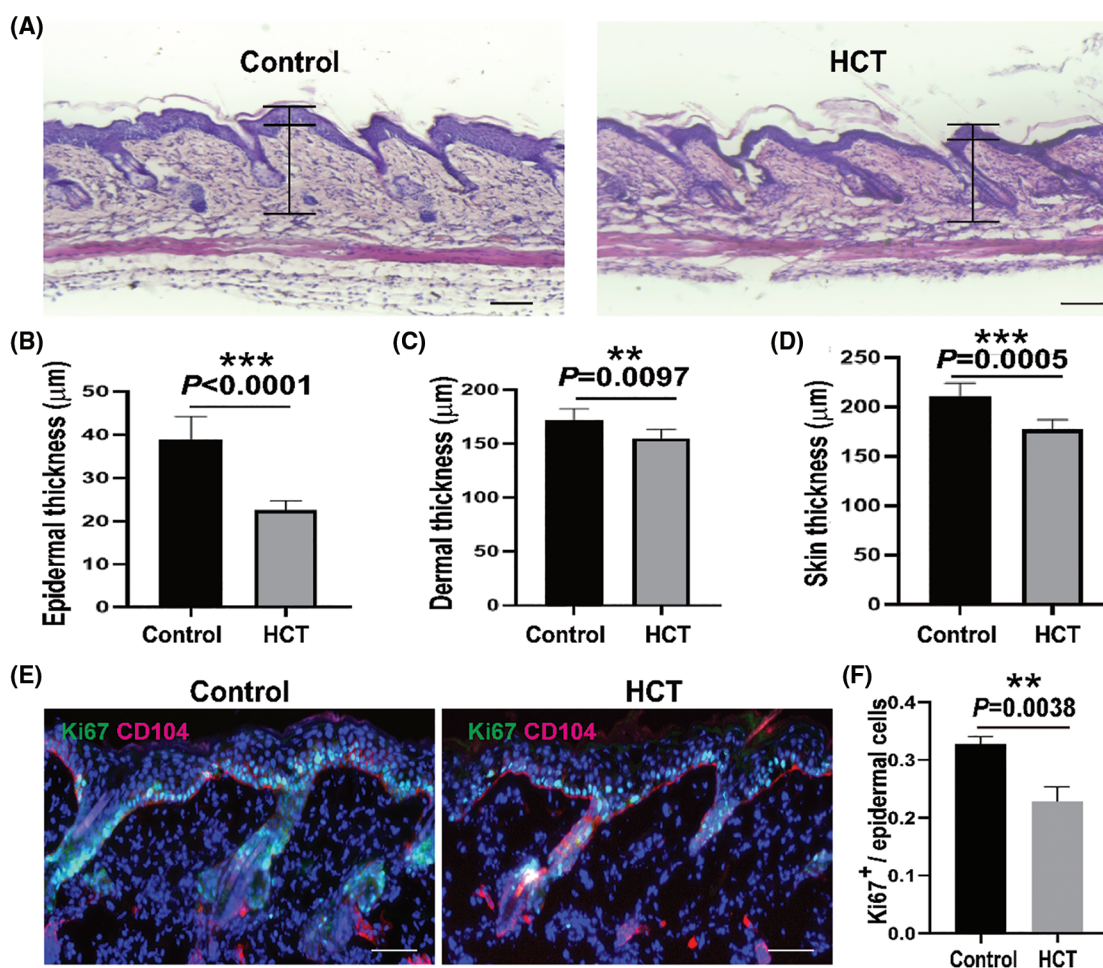


Figure 3: HCT treatment suppresses inflammation-mediated skin thickening induced by TPA. TPA treatment causes thickened back skin. (A) Representative images of H&E staining of back skin from control groups and HCT groups. The epidermal and dermal thickness was indicated in the images. (B-D) Statistic quantification of epidermal (B), dermal (C) and whole skin (D) thickness of control groups and HCT groups. N = 6. (E) Representative images of immunofluorescent staining of back skin from control groups and HCT groups using proliferation marker (Ki67, green) and basal membrane marker (CD104, red). (F) Statistic quantification of Ki67⁺ cells in interfollicular epidermis. N = 3. Scale bar for (A) and (E), 100 μ m. (**) represents $P < 0.01$, (***) represents $P < 0.001$

3.4 HCT Treatment Reduces Tumor-Infiltrating T Cells

Since HCT is capable of reducing immune cells infiltrated into inflammatory tissues [33,34], we then investigated whether HCT affects tumor microenvironments and examined tumor-infiltrating T cells, which are recognized as the main effectors of antitumor immune responses [41]. Western blot analysis showed that the surface protein markers CD4 and CD8 of T cells were largely diminished in HCT treated tumors (Fig. 4A). Immunostaining analysis showed that there were abundant CD8⁺ cytotoxic T cells and the CD4⁺ helper T cells infiltrated into cutaneous SCC tissues, especially in the stroma compartment (Fig. 4B). HCT treatment reduced both of these two types of T cells. The CD4⁺ helper T cells number was reduced much more than that of the CD8⁺ cytotoxic T cells after HCT treatment (Figs. 4B and 4C).

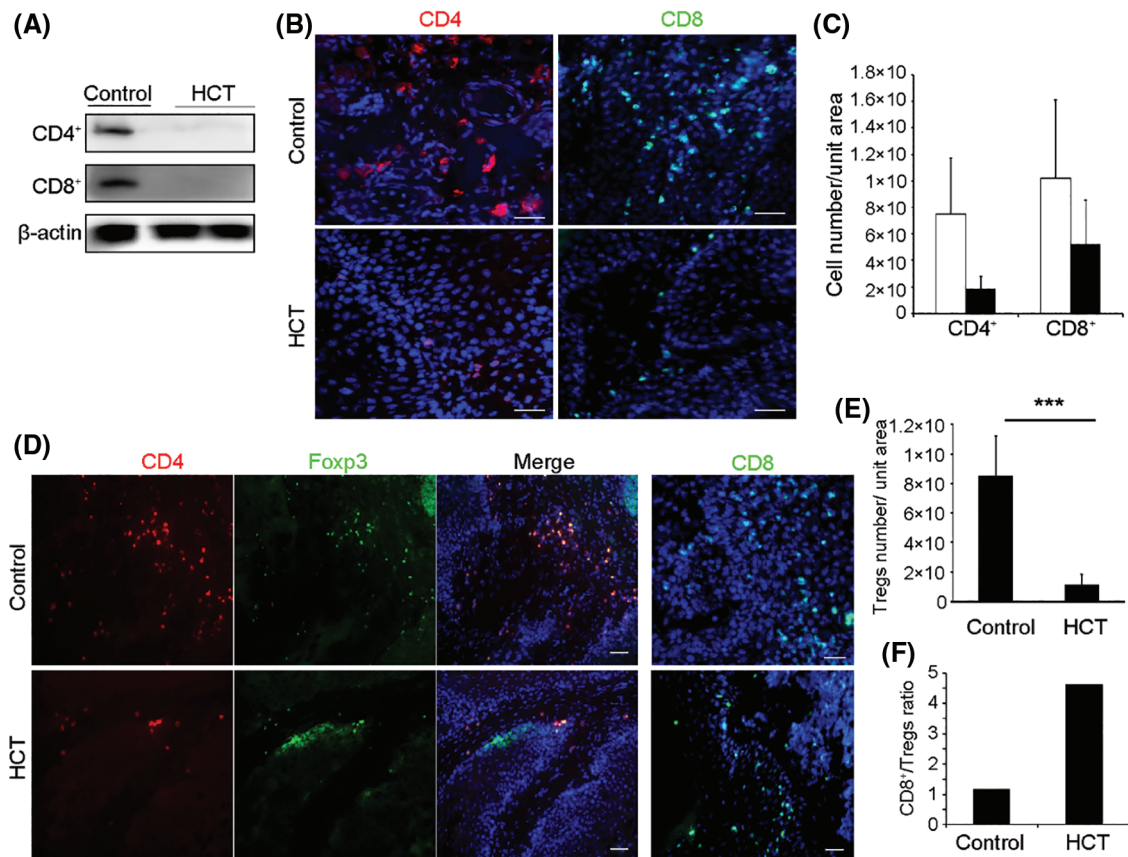


Figure 4: HCT treatment reduces tumor-infiltrating T lymphocytes and increases the ratio of the CD8⁺/Treg cell. (A) HCT treatment reduced the expression of CD4 and CD8 proteins in tumor samples, as analyzed by Western blot. (B) Representative immunofluorescence images of tumor-infiltrating CD4⁺ and CD8⁺ cells. Frozen tumors samples were immunostained with Alexa Fluor 700 conjugated anti-CD4 antibody or Alexa Fluor 488 conjugated anti-CD8 antibody. (C) Statistic quantification of CD4⁺ and CD8⁺ cells number. All fields of CD4⁺ or CD8⁺ cells in several sections from each tumor were counted. N=4 mice. For CD4⁺ cells, $P=0.058$; For CD8⁺ cells, $P=0.210$. Scale bar, 50 μ m. (D) Representative immunofluorescence images of CD4⁺, Foxp3⁺ Treg cells and CD8⁺ effector T cells in the tumors. Tumor samples were co-immunostained with Alexa Fluor 700 conjugated anti-CD4 antibody together with Alexa Fluor 488 conjugated anti-Foxp3 antibodies, or immunostained with Alexa Fluor 488 conjugated anti-CD8 antibody (right panel). Scale bar, 50 μ m. (E) Statistic quantification of CD4⁺, Foxp3⁺ Tregs number. All fields of CD4⁺, Foxp3⁺ Tregs in several sections from each tumor were counted. N=8 mice. $P=0.0002$. (F) The ratio of CD8⁺ effector T cells number to CD4⁺, Foxp3⁺ Tregs number. (***) represents $P < 0.001$

3.5 HCT Treatment Significantly Increases the Ratio of the CD8⁺/Treg Cells

CD4⁺ T cells can be subdivided into regulatory T cells (Tregs) and traditional help T cells. Tregs, formerly known as suppressor T cells, suppress induction and proliferation of cytotoxic T cells, T helper cells and Antigen-Presenting Cells (APCs), therefore are detrimental to anti-tumor immune responses [42]. Tregs express the biomarker transcription factor Foxp3. Immunostaining results showed that most of the CD4⁺ cells in tumors were Foxp3⁺ Tregs, and that CD4⁺, Foxp3⁺ Tregs number was significantly decreased after HCT treatment (Figs. 4D and 4E). In addition, the ratio of the CD8⁺/Treg cells increased by about 4 folds after HCT treatment (Fig. 4F).

3.6 HCT Treatment on SCC Cells Reduces mRNA Expression of Inflammatory Factors

To investigate the molecular mechanism of why skin inflammation, as well as tumor-infiltrating T cells, were reduced after HCT treatment, we examined the mRNA expression level of inflammatory factors in SCC cell line A431 treated by HCT *in vitro*. The real-time quantitative PCR analysis showed that the mRNA expression of IL-1 β , IL-6 and TNF- α was only 11%, 8% and 19% of the control group, respectively (Fig. 5). These results indicate that HCT treatment might reduce the expression of inflammatory factors in skin cells, therefore reducing the recruitment of inflammatory cells, preventing skin tumorigenesis and suppressing SCC growth.

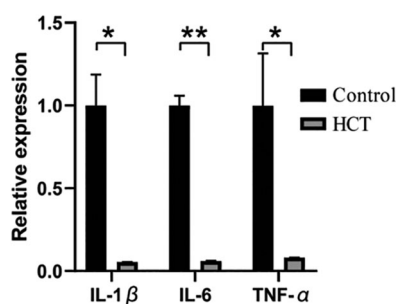


Figure 5: HCT treatment on SCC cells reduces mRNA expression of inflammatory factors. The mRNA expression of IL-1 β , IL-6 and TNF- α in human A431 cells after HCT treatment was measured by real-time quantitative PCR. Each gene expression level from the control group was normalized as 1. For IL-1 β , $P=0.0127$; for IL-6, $P=0.0012$; for TNF- α , $P=0.037$. $N=3$. (*) represents $P<0.05$ and (**) represents $P<0.01$.

4 Discussion

In this work, we evaluated the anti-cancer activity of HCT and its bioactive ingredient *in vivo* using the DMBA/TPA-induced cutaneous SCC model. We have demonstrated that topical application of HCT reduces tumor-infiltrating T lymphocytes, especially Tregs, increases CD8⁺/Treg cells ratio and efficiently suppresses tumor growth without obvious toxicity.

DMBA/TPA induced mice SCC is a unique *in vivo* cancer model, in which tumors on back skin can be directly visualized, quantitatively measured and traced individually over time. Since SCC has all of the hallmarks of cancer development, including DNA mutation, genome instability, epigenetic changes, inflammation, oxidative stress and tumor microenvironment changes [24–27], our study not only demonstrates the anti-cancer activity of HCT on SCC *in vivo*, but more broadly, indicates HCT might have general anti-cancer activity on other cancer types *in vivo*.

Chemical-induced SCC might develop through activating different cancer-promoting pathways which are originated from different DNA mutations [29]. Therefore, it is no surprise that there is huge heterogeneity of protein expression levels between tumors, either from different mice or the same mouse.

It is difficult to conclude which cancer-promoting pathways are altered by HCT treatment, unless a huge number of tumors are statistically analyzed.

HCT possesses anti-inflammatory activity [1,2], and it can reduce inflammatory cell infiltration in different animal inflammation models [33,34]. HCT treatment reverses oxaliplatin-induced neuropathic pain in the rat by regulating Th17/Treg balance [43]. Consistent with previous reports, tumor-infiltrating lymphocytes especially Tregs largely decrease, and the CD8⁺/Treg cells ratio increases after HCT treatment. Since Tregs dampen anti-cancer immune response through negatively regulating activation of effector T cells, the significant increase of CD8⁺/Treg cells ratio by HCT treatment can at least partially explain why HCT exhibits anti-cancer activity. In addition, a change of infiltrating lymphocytes in tumors by HCT treatment indicates HCT might be able to change inflammatory cell infiltration during the early stage of cancer development, therefore affecting another process of cancer development. This was supported by the data that HCT pretreatment reduced the skin thickening/inflammation induced by TPA alone.

Since we topically applied the drug onto the tumor, it seems unlikely that HCT modulates the whole immune system and then affects the tumor-infiltrating immune cells. Instead, our results support that HCT active components might penetrate tumor tissue and directly impact the cancer cells and immune cells around. Mechanistically, we have found that direct treatment of SCC cells *in vitro* by HCT could reduce the mRNA expression of IL-1 β , IL-6 and TNF- α from SCC cells. This indicates that HCT might prevent skin tumorigenesis and suppress SCC growth by reducing the expression of inflammatory factors secreted from skin cells and therefore reducing the recruitment of inflammatory cells, including T lymphocytes. Thus, HCT treatment might represent a novel immune therapy, like other therapies under development, for treating cancers [44,45].

HCT possesses activities against inflammation, oxidative stress and DNA mutations. All of these events are interconnected and play important roles in the initiation and progression of cutaneous SCC. Although a decrease of tumor-infiltrating Tregs and an increase of CD8⁺/Treg cells ratio can explain the anti-cancer activity of HCT, we cannot exclude that other activities of HCT might also contribute to these anti-cancer effects. Nevertheless, our study provides another insight into the molecular mechanism of HCT anti-cancer activity: it can re-balance the lymphocytes effector and suppressor infiltrated into the tumor, therefore modulating the tumor immune microenvironment to counteract cancer cells.

5 Conclusions

In summary, our work demonstrates the therapeutic effects of HCT and its bioactive ingredients SNH on cutaneous SCC and reveals that HCT might inhibit cancer through regulating tumor-infiltrating lymphocytes and the tumor immune microenvironments. Understanding the molecular mechanism of HCT against tumorigenesis may facilitate the development of new topical agents from HCT for the treatment of cutaneous SCC and other cancers. The anti-inflammatory effects of HCT by balancing the lymphocytes effector and suppressor infiltrated in the tissues might also help to explain/illustrate the mechanism of HCT in other diseases including anti-SARS-CoV-2 activity.

Authorship: Conceptualization: Liao, Gao, Huang and Wang. Study design and execution: Gao, Gui, Zheng and Wang. Data analysis: Gao, Gui, Zheng, Wang, Wang and Gong. Writing: Liao and Gao.

Ethics Approval: This article does not contain any studies with human participants. All experiments involving animals were performed following the guidelines of the Institutional Animal Care and Use Committee (IACUC) of Shanghai University (the Protocol No: 2019033).

Acknowledgement: We thank Lichun Jiang at the Shanghai Tech University for helping us edit the manuscript.

Funding Statement: This work was supported by the National Natural Science Foundation of China (81903054, 81972563), and the United Fujian Provincial Health and Education Project for Tackling the Key Research (WKJ2016-2-34).

Conflicts of Interest: The authors declare that they have no conflicts of interest to report regarding the present study.

References

1. Kumar, M., Prasad, S. K., Hemalatha, S. (2014). A current update on the phytopharmacological aspects of *Houttuynia cordata Thunb.* *Pharmacognosy Reviews*, 8(15), 22–35. DOI 10.4103/0973-7847.125525.
2. Fu, J., Dai, L., Lin, Z., Lu, H. (2013). *Houttuynia cordata Thunb.*: A review of phytochemistry and pharmacology and quality control. *Chinese Medicine*, 4(3), 101–123. DOI 10.4236/cm.2013.43015.
3. Das, S. K., Mahanta, S., Tanti, B., Tag, H., Hui, P. K. (2021). Identification of phytochemicals from *Houttuynia cordata Thunb* as potential inhibitors for SARS-CoV-2 replication proteins through GC-MS/LC-MS characterization, molecular docking and molecular dynamics simulation. *Molecular Diversity*, 26(1), 365–388. DOI 10.1007/s11030-021-10226-2.
4. Remali, J., Aizat, W. M. (2020). A review on plant bioactive compounds and their modes of action against coronavirus infection. *Frontiers in Pharmacology*, 11, 589044. DOI 10.3389/fphar.2020.589044.
5. Bahadur Gurung, A., Ajmal Ali, M., Lee, J., Abul Farah, M., Mashay Al-Anazi, K. et al. (2021). Identification of SARS-CoV-2 inhibitors from extracts of *Houttuynia cordata Thunb.* *Saudi Journal of Biological Sciences*, 28(12), 7517–7527. DOI 10.1016/j.sjbs.2021.08.100.
6. Tang, Y. J., Yang, J. S., Lin, C. F., Shyu, W. C., Tsuzuki, M. et al. (2009). *Houttuynia cordata Thunb* extract induces apoptosis through mitochondrial-dependent pathway in HT-29 human colon adenocarcinoma cells. *Oncology Reports*, 22(5), 1051–1056.
7. Liu, J., Zhu, X., Yang, D., Li, R., Jiang, J. (2020). Effect of heat treatment on the anticancer activity of *Houttuynia cordata Thunb* aerial stem extract in human gastric cancer SGC-7901 cells. *Nutrition and Cancer*, 73(1), 160–168.
8. Yanarajana, M., Nararatwanchai, T., Thairat, S., Tancharoen, S. (2017). Antiproliferative activity and induction of apoptosis in human melanoma cells by *Houttuynia cordata Thunb* extract. *Anticancer Research*, 37(12), 6619–6628.
9. Kim, J. M., Hwang, I. H., Jang, I. S., Kim, M., Bang, I. S. et al. (2017). *Houttuynia cordata Thunb* promotes activation of HIF-1A-FOXO3 and MEF2A pathways to induce apoptosis in human HepG2 hepatocellular carcinoma cells. *Integrative Cancer Therapies*, 16(3), 360–372. DOI 10.1177/1534735416670987.
10. Subhawa, S., Chewonarin, T., Banjerdpongchai, R. (2020). The effects of *Houttuynia cordata Thunb* and piper ribesiodides wall extracts on breast carcinoma cell proliferation, migration, invasion and apoptosis. *Molecules*, 25(5), 1196. DOI 10.3390/molecules25051196.
11. Lai, K. C., Chiu, Y. J., Tang, Y. J., Lin, K. L., Chiang, J. H. et al. (2010). *Houttuynia cordata Thunb* extract inhibits cell growth and induces apoptosis in human primary colorectal cancer cells. *Anticancer Research*, 30(9), 3549–3556.
12. Chen, Y. F., Yang, J. S., Chang, W. S., Tsai, S. C., Peng, S. F. et al. (2013). *Houttuynia cordata Thunb* extract modulates G0/G1 arrest and Fas/CD95-mediated death receptor apoptotic cell death in human lung cancer a549 cells. *Journal of Biomedical Science*, 20, 18. DOI 10.1186/1423-0127-20-18.
13. Kwon, K. B., Kim, E. K., Shin, B. C., Seo, E. A., Yang, J. Y. et al. (2003). Herba houttuyniae extract induces apoptotic death of human promyelocytic leukemia cells via caspase activation accompanied by dissipation of mitochondrial membrane potential and cytochrome c release. *Experimental & Molecular Medicine*, 35(2), 91–97. DOI 10.1038/emm.2003.13.
14. Lou, Y., Guo, Z., Zhu, Y., Kong, M., Zhang, R. et al. (2019). *Houttuynia cordata Thunb.* and its bioactive compound 2-undecanone significantly suppress benzo(a)pyrene-induced lung tumorigenesis by activating the nrf2-HO-1/NQO-1 signaling pathway. *Journal of Experimental & Clinical Cancer Research*, 38(1), 242. DOI 10.1186/s13046-019-1255-3.
15. Leiter, U., Eigentler, T., Garbe, C. (2014). Epidemiology of skin cancer. *Advances in Experimental Medicine and Biology*, 810, 120–140. DOI 10.1007/978-1-4939-0437-2.
16. Gandhi, S. A., Kampp, J. (2015). Skin cancer epidemiology, detection, and management. *The Medical Clinics of North America*, 99(6), 1323–1335. DOI 10.1016/j.mcna.2015.06.002.

17. Apalla, Z., Nashan, D., Weller, R. B., Castellsague, X. (2017). Skin cancer: Epidemiology, disease burden, pathophysiology, diagnosis, and therapeutic approaches. *Dermatology and Therapy*, 7(Suppl 1), 5–19. DOI 10.1007/s13555-016-0165-y.
18. Brancaccio, G., Briatico, G., Pellegrini, C., Rocco, T., Moscarella, E. et al. (2021). Risk factors and diagnosis of advanced cutaneous squamous cell carcinoma. *Dermatology Practical & Conceptual*, 11(Suppl 2), e2021166S. DOI 10.5826/dpc.11S2a166S.
19. Agar, N. J., Kirton, C., Patel, R. S., Martin, R. C., Angelo, N. et al. (2015). Predicting lymph node metastases in cutaneous squamous cell carcinoma: Use of a morphological scoring system. *The New Zealand Medical Journal*, 128(1411), 59–67.
20. Verzi, A. E., Lacarrubba, F., Caltabiano, R., Broggi, G., Musumeci, M. L. et al. (2019). Reflectance confocal microscopy features of plaque psoriasis overlap with horizontal histopathological sections: A case series. *The American Journal of Dermatopathology*, 41(5), 355–357. DOI 10.1097/DAD.0000000000001297.
21. Broggi, G., Verzi, A. E., Caltabiano, R., Micali, G., Lacarrubba, F. (2021). Correlation between in vivo reflectance confocal microscopy and horizontal histopathology in skin cancer: A review. *Frontiers in Oncology*, 11, 653140. DOI 10.3389/fonc.2021.653140.
22. Broggi, G., Verzi, A. E., Lacarrubba, F., Caltabiano, R., di Natale, A. et al. (2020). Correlation between reflectance confocal microscopy features and horizontal histopathology in cutaneous squamous cell carcinoma *in situ*: A case series. *Journal of Cutaneous Pathology*, 47(8), 777–780. DOI 10.1111/cup.13708.
23. Fahradyan, A., Howell, A. C., Wolfswinkel, E. M., Tsuha, M., Sheth, P. et al. (2017). Updates on the management of non-melanoma skin cancer (NMSC). *Healthcare*, 5(4), 82. DOI 10.3390/healthcare5040082.
24. Voiculescu, V., Calenic, B., Ghita, M., Lupu, M., Caruntu, A. et al. (2016). From normal skin to squamous cell carcinoma: A quest for novel biomarkers. *Disease Markers*, 2016, 4517492. DOI 10.1155/2016/4517492.
25. Parekh, V., Seykora, J. T. (2017). Cutaneous squamous cell carcinoma. *Clinics in Laboratory Medicine*, 37(3), 503–525. DOI 10.1016/j.cll.2017.06.003.
26. Nissinen, L., Farshchian, M., Riihila, P., Kahari, V. M. (2016). New perspectives on role of tumor microenvironment in progression of cutaneous squamous cell carcinoma. *Cell and Tissue Research*, 365(3), 691–702. DOI 10.1007/s00441-016-2457-z.
27. Marks, F., Furstenberger, G. (1986). Experimental evidence that skin carcinogenesis is a multistep phenomenon. *The British Journal of Dermatology*, 115(Suppl 31), 1–8. DOI 10.1111/j.1365-2133.1986.tb02100.x.
28. Abel, E. L., Angel, J. M., Kiguchi, K., DiGiovanni, J. (2009). Multi-stage chemical carcinogenesis in mouse skin: Fundamentals and applications. *Nature Protocols*, 4(9), 1350–1362. DOI 10.1038/nprot.2009.120.
29. Nassar, D., Latil, M., Boeckx, B., Lambrechts, D., Blanpain, C. (2015). Genomic landscape of carcinogen-induced and genetically induced mouse skin squamous cell carcinoma. *Nature Medicine*, 21(8), 946–954. DOI 10.1038/nm.3878.
30. Reagan-Shaw, S., Nihal, M., Ahmad, N. (2008). Dose translation from animal to human studies revisited. *The FASEB Journal*, 22(3), 659–661. DOI 10.1096/fj.07-9574LSF.
31. Balkwill, F. R., Capasso, M., Hagemann, T. (2012). The tumor microenvironment at a glance. *Journal of Cell Science*, 125(23), 5591–5596. DOI 10.1242/jcs.116392.
32. Kareva, I. (2019). Metabolism and gut microbiota in cancer immunoediting, CD8/Treg ratios, immune cell homeostasis, and cancer (Immuno) therapy: Concise review. *Stem Cells*, 37(10), 1273–1280. DOI 10.1002/stem.3051.
33. Kim, D., Park, D., Kyung, J., Yang, Y. H., Choi, E. K. et al. (2012). Anti-inflammatory effects of houttuynia cordata supercritical extract in carrageenan-air pouch inflammation model. *Laboratory Animal Research*, 28(2), 137–140. DOI 10.5625/lar.2012.28.2.137.
34. Ling, L. J., Lu, Y., Zhang, Y. Y., Zhu, H. Y., Tu, P. et al. (2020). Flavonoids from houttuynia cordata attenuate H1N1-induced acute lung injury in mice via inhibition of influenza virus and toll-like receptor signalling. *Phytomedicine: International Journal of Phytotherapy and Phytopharmacology*, 67, 153150. DOI 10.1016/j.phymed.2019.153150.
35. Liu, X., Zhong, L., Xie, J., Sui, Y., Li, G. et al. (2021). Sodium houttuynfonate: A review of its antimicrobial, anti-inflammatory and cardiovascular protective effects. *European Journal of Pharmacology*, 902, 174110. DOI 10.1016/j.ejphar.2021.174110.

36. Malanchi, I., Peinado, H., Kassen, D., Hussenet, T., Metzger, D. et al. (2008). Cutaneous cancer stem cell maintenance is dependent on beta-catenin signalling. *Nature*, 452(7187), 650–653. DOI 10.1038/nature06835.
37. Spencer, J. M., Kahn, S. M., Jiang, W., DeLeo, V. A., Weinstein, I. B. (1995). Activated ras genes occur in human actinic keratoses, premalignant precursors to squamous cell carcinomas. *Archives of Dermatology*, 131(7), 796–800. DOI 10.1001/archderm.1995.01690190048009.
38. Pierceall, W. E., Goldberg, L. H., Tainsky, M. A., Mukhopadhyay, T., Ananthaswamy, H. N. (1991). Ras gene mutation and amplification in human nonmelanoma skin cancers. *Molecular Carcinogenesis*, 4(3), 196–202. DOI 10.1002/(ISSN)1098-2744.
39. Inoue, H., Mori, T., Shibata, S., Koshihara, Y. (1989). Modulation by glycyrrhetic acid derivatives of TPA-induced mouse ear oedema. *British Journal of Pharmacology*, 96(1), 204–210. DOI 10.1111/j.1476-5381.1989.tb11801.x.
40. Kang, M. R., Jo, S. A., Lee, H., Yoon, Y. D., Kwon, J. H. et al. (2020). Inhibition of skin inflammation by scytonemin, an ultraviolet sunscreen pigment. *Marine Drugs*, 18(6), 300. DOI 10.3390/md18060300.
41. Yu, P., Fu, Y. X. (2006). Tumor-infiltrating T lymphocytes: Friends or foes? *Laboratory Investigation*, 86(3), 231–45. DOI 10.1038/labinvest.3700389.
42. Knutson, K. L., Disis, M. L. (2005). Tumor antigen-specific T helper cells in cancer immunity and immunotherapy. *Cancer Immunology, Immunotherapy*, 54(8), 721–728. DOI 10.1007/s00262-004-0653-2.
43. Wan, C. F., Zheng, L. L., Liu, Y., Yu, X. (2016). *Houttuynia cordata* Thunb reverses oxaliplatin-induced neuropathic pain in rat by regulating Th17/Treg balance. *American Journal of Translational Research*, 8(3), 1609–1614.
44. Blázquez-castro, A., Stockert, J. C. (2021). Biomedical overview of melanin. 1. Updating melanin biology and chemistry, physico-chemical properties, melanoma tumors, and photothermal therapy. *BIOCELL*, 45(4), 849–862. DOI 10.32604/biocell.2021.015900.
45. Lu, P., Hill, H. A., Navsaria, L. J., Wang, M. L. (2021). CAR-T and other adoptive cell therapies for B cell malignancies. *Journal of the National Cancer Center*, 1(3), 88–96. DOI 10.1016/j.jncc.2021.07.001.